Sheffield Hallam University

Discrimination of papillary thyroid cancer from non-cancerous thyroid tissue based on lipid profiling by mass spectrometry imaging

WOJAKOWSKA, A, COLE, Laura <http://orcid.org/0000-0002-2538-6291>, CHEKAN, M, BEDNARCZYK, K, MAKSYMIAK, M, OCZKO-WOJCIECHOWSKA, M, JARZĄB, B, CLENCH, Malcolm <http://orcid.org/0000-0002-0798-831X>, POLAŃSKA, J, PIETROWSKA, M and WIDLAK, P

Available from Sheffield Hallam University Research Archive (SHURA) at:

http://shura.shu.ac.uk/23068/

This document is the author deposited version. You are advised to consult the publisher's version if you wish to cite from it.

Published version

Copyright and re-use policy

Discrimination of papillary thyroid cancer from non-cancerous thyroid tissue based on lipid profiling by mass spectrometry imaging

Odróżnienie brodawkowatego raka tarczycy od tkanki nienowotworowej w oparciu o profilowanie lipidów metodą MALDI-MSI

Anna Wojakowska[1], Laura M. Cole[2], Mykola Chekan[1], Katarzyna Bednarczyk[3], Magdalena Maksymiak[1], Małgorzata Oczko-Wojciechowska[1], Barbara Jarząb[1], Malcolm R. Clench[2], Joanna Polańska[3], Monika Pietrowska[1], Piotr Widlak[1]

[1]*Maria Sklodowska-Curie Institute — Oncology Center, Gliwice Branch, Gliwice, Poland*
[2]*Centre for Mass Spectrometry Imaging, Biomolecular Sciences Research Centre, Sheffield Hallam University, Sheffield, United Kingdom*
[3]*Silesian University of Technology, Gliwice, Poland*

Abstract

Introduction: The distinction of papillary thyroid carcinomas from benign thyroid lesions has important implication for clinical management. Classification based on histopathological features can be supported by molecular biomarkers, including lipidomic signatures, identified with the use of high-throughput mass spectrometry techniques. Formalin fixation is a standard procedure for stabilization and preservation of tissue samples, therefore this type of samples constitute highly valuable source of clinical material for retrospective molecular studies. In this study we used mass spectrometry imaging to detect lipids discriminating papillary cancer from not cancerous thyroid directly in formalin-fixed tissue sections.
Material and methods: For this purpose imaging and profiling of lipids present in non-malignant and cancerous thyroid tissue specimens were conducted. High resolution MALDI-Q-Ion Mobility-TOF-MS technique was used for lipidomic analysis of formalin fixed thyroid tissue samples. Lipids were identified by the comparison of the exact molecular masses and fragmentation pathways of the protonated molecule ions, recorded during the MS/MS experiments, with LIPID MAPS database.
Results: Several phosphatidylcholines (32:0, 32:1, 34:1 and 36:3), sphingomyelins (34:1 and 36:1) and phosphatidic acids (36:2 and 36:3) were detected and their abundances were significantly higher in cancerous tissue compared to non-cancerous tissue. The same lipid species were detected in formalin-fixed as in fresh-frozen tissue, but [M + Na]$^+$ ions were the most abundant in formalin fixed whereas [M + K]$^+$ ions were predominant in fresh tissue.
Conclusions: Our results prove the viability of MALDI-MSI for analysis of lipid distribution directly in formalin-fixed tissue, and the potential for their use in the classification of thyroid diseases. **(Endokrynol Pol 2018; 69 (1): 2–8)**

Key words: *mass spectrometry imaging, papillary thyroid carcinoma, clinical lipidomics, formalin-fixed tissue specimens*

Streszczenie

Wstęp: Rozróżnienie brodawkowatych raków tarczycy od łagodnych zmian tarczycy ma istotny wpływ na postepowanie kliniczne. Klasyfikacja w oparciu o cechy histopatologiczne może być wspomagana biomarkerami molekularnymi, w tym składnikami lipidowymi, zidentyfikowanymi przy użyciu wysokorozdzielczych technik spektrometrii masowej. Utrwalanie tkanki w formalinie jest standardową procedurą stabilizacji i konserwacji tkanek, które stanowią cenne źródło materiału klinicznego w retrospektywnych badaniach molekularnych. W prezentowanych badaniach wykorzystano obrazowanie molekularne metodą MALDI w celu wykrycia składników lipidomu, obecnych w tkankach utrwalonych w formalinie, różnicujących raka brodawkowatego od tarczycy nienowotworowej.
Materiał i metody: W tym celu przeprowadzono obrazowanie i profilowanie lipidów obecnych w próbkach tkanek tarczycy zmienionej nowotworowo i nienowotworowej. Do analizy lipidomicznej tkanek tarczycy utrwalonych w formalinie zastosowano wysokorozdzielczą technikę MALDI-Q-Ion Mobility-TOF-MS. Składniki lipidowe zostały zidentyfikowane przez porównanie uzyskanych dokładnych mas cząsteczkowych i szlaków fragmentacji jonów protonowanych, zarejestrowanych podczas eksperymentów MS/MS, z bazą danych LIPID MAPS.
Wyniki: W oparciu o przeprowadzone analizy wykryto lipidy należące do klas fosfatydylocholin (32:0, 32:1, 34:1 i 36:3), sfingomielin (34:1 i 36:1) i kwasów fosfatydowych (36:2 i 36:3), a ich ilość była znacząco wyższa w tkance nowotworowej w porównaniu z tarczycą nienowotworową. Te same składniki lipidowe wykryto w preparatach utrwalonych w formalinie, jak i w tkance świeżo mrożonej, przy czym jony [M + Na]+ obecne były w przewadze w tkance utrwalonej w formalinie, podczas gdy w świeżej tkance przeważały jony [M + K]+.
Wnioski: Prezentowane wyniki potwierdzają możliwości wykorzystania techniki MALDI-MSI w analizie dystrybucji lipidów bezpośrednio w tkankach stabilizowanych formaliną oraz dają nadzieję na potencjalne wykorzystanie ich w klasyfikacji chorób tarczycy.
(Endokrynol Pol 2018; 69 (1): 2–8)

Słowa kluczowe: *obrazowanie metodami spektrometrii masowej, brodawkowaty rak tarczycy, lipidomika kliniczna, próbki tkanek stabilizowane formaliną*

✉ Piotr Widlak M.D., Ph.D., Maria Sklodowska-Curie Institute — Oncology Center, Wybrzeże Armii Krajowej St. 15, 44–101 Gliwice, tel.: +48 32 278 96 72, fax: +48 32 278 98 40, e-mail: piotr.widlak@io.gliwice.pl

Introduction

Papillary thyroid carcinomas (PTC) are the most common thyroid cancers and constitute more than 70% of all thyroid malignancies [1]. Classification of thyroid lesion is critical for prognosis and treatment selection, hence the distinction of PTC from other malignant and benign thyroid lesions has important implications for clinical management. Diagnosis of PTC is based on its histological pattern involving specific papillary architecture, yet some papillary carcinomas show not the typical histological features [2, 3]. Moreover, diagnosis of thyroid cancers is initially based on the fine needle aspiration cytology of thyroid nodules [4]. However, morphology-based methods have several limitations restricting correct classification of cancer subtypes [5, 6]. Hence, classification of different thyroid cancer subtypes could be facilitated if histological/cytological patterns were supported by molecular biomarkers.

Lipids are among classes of biomolecules with a high potential value in cancer diagnostics [7]. Phospholipids, which are the major constituents of cell membranes, play an important role in signal transduction, inflammation, cell proliferation and differentiation [8–10], and influence key aspects of cancer phenotype [11, 12]. A few papers have reported differences in the lipid profiles of thyroid neoplasms [13–16], hence this class of compounds could be potentially implemented in classification of thyroid lesions. Mass spectrometry imaging (MSI) is a newly developed technique allowing for determination of spatial distribution of metabolites and lipids within the tissue sections [17–20]. An important advantage of molecular profiling by MSI lays on its ability to use spectra exported from specific tissue areas defined by a pathologist based on their morphological features, which might be called a "virtual microdissection". Formalin fixation (FF) is a standard procedure for stabilization and preservation of tissue specimens for clinical purposes. However, fixation process impairs the ability to analyse certain classes of biomolecules [21, 22]. Recently, we demonstrated that tissues fixed with formalin and processed without paraffin embedding were suitable for imaging of lipids by MALDI (matrix-assisted laser-desorption ionization)-MSI [23]. In the present study this approach was used for profiling of lipids in FF tissue to detect species discriminating PTC from non-cancerous thyroid.

Material and methods

Clinical material

Tissue samples were collected from 3 Caucasian patients with PTC treated in Maria Sklodowska-Curie Institute (Gliwice, Poland). Samples were obtained from a cancer and adjacent non-cancerous thyroid tissue immediately after tumour resection. Detailed information on clinical samples is given in the Supplementary Table sI. Immediately after resection tissue specimens were fixed in neutral buffered formalin (4% formaldehyde in phosphate buffer, pH 7.0) for 24 hours at room temperature, and stored in –80°C until analysed. Some of the tissue samples were also frozen in liquid nitrogen.

Tissue sample preparation and matrix deposition

Ten μm thick tissue sections were prepared using a cryostat, and then serial sections were mounted onto indium tin oxide (ITO) either coated glass slides (Bruker, Germany) for MSI or standard glass slides for hematoxylin and eosin (H&E) staining. Each tissue section for MSI was washed twice with distilled water (2 × 30 seconds), and then covered with α-cyano-4-hydroxycinnamic acid (CHCA) matrix solution (0.5% α-cyano-4-hydroxycinnamic acid in 70% methanol and 0.2% trifluoroacetic acid) in a series of 4 layers (5 μL/min) using SunCollect Instrument (SunChrom, Germany).

Mass spectrometry analysis

Mass spectrometry imaging was performed using a HDMS SYNAPT TM G2 system and Driftscope 2.1 software (Waters, UK). Mass spectrometry (MS) and tandem mass spectrometry (MS/MS) data were acquired in positive ion sensitivity mode at a mass resolution of 10 000 full width at half maximum (FWHM) with ion mobility separation enabled and over the mass range m/z 100 to 1200. Image acquisition was performed using raster imaging mode at 100 μm spatial resolution, Biomap 3.7.5.5 software (http://www.maldi-msi.org/) was used for image generation. The MS/MS spectra were acquired manually moving the laser position and adjusting the collision energy to achieve good signal to noise for product ions across the full m/z range of the spectrum. Collision energies were adjusted from 25 to 40 eV during acquisition and acquisition times were generally of the order of 5–10 s per spectrum. Lipids were identified by the comparison of the exact molecular masses and fragmentation pathways of the protonated molecule ions, recorded during the MS/MS experiments, with LIPIDMAPS database (www.lipidmaps.org) Positive identification of molecular ions was assumed if a unique match with error below 3 ppm was found.

Statistical analysis

Mass spectra were pre-processed and spectral components were detected using the Gaussian Mixture Model as described in details elsewhere [24]. Due to significant deviations from normal distribution the non-parametric Kruskal-Wallis ANOVA was used to check

Table I. *Numbers of spectral components differentiating compared ROIs*

Tabela I. *Liczba różnicujących składników widm w oparciu o porównanie obszarów ROI*

	CTR-1	CTR-2	CTR-3	CAN-1	CAN-2	CAN-3
CTR-1	x	257	286	254	219	209
CTR-2		x	299	183	205	272
CTR-3			x	275	299	227
CAN-1				x	198	249
CAN-2					x	249
CAN-3						x

Presented are numbers of spectral components that showed significantly different abundances (corrected p-value < 0.05 and effect size > 0.8) between all ROIs compared pairwise; CTR — non-cancerous (control); CAN — cancer; 1,2,3 — patients numbers

equality of location statistics among populations of spectra (the Benjamini-Hochberg correction for multiple testing was applied). The post hoc multiple pairwise comparisons were done by Dunn's test. The results of statistical testing were supported by estimation of the pairwise Wilcox-Tian's effect size; the effects above 0.8 with appropriate pairwise comparison p-value less than 0.05 were considered significantly large.

Results

Cancer and non-cancerous regions of interest (ROIs) were defined by a pathologist in the tissue specimen from each patient and 100 spectra were imported from each ROI (average mass spectra from each ROI are presented in Fig. 1); 476 components representing molecular species with their isotopic envelopes were detected in the 700–900 Da mass range. For each pair of ROIs the statistical significance of differences in abundance of each spectral component was estimated (numbers of differentiating components are listed in Table I). The average number of differentiating components between paired cancer and noncancerous ROIs was 229. On the other hand, average number of differentiating components among all cancer ROIs was 232, while average number of differentiated components among all non-cancerous ROIs was 281. This might suggest a higher degree of similarity among PTC from different patients than among non-cancerous thyroid regions from different patients. However, this unexpected observation could be explained when considering that "non-cancerous" regions include one "normal" thyroid tissue (Patient_2) and two non-cancerous thyroid diseases: nodular goiter (Patient_1) and lymphocytic thyroiditis (Patient_3). Nevertheless, when the overlap of cancer-upregulated or downregulated components between three different patients were analysed 33 commonly upregulated and 23 commonly downregulated components were detected. Furthermore, when combined spectra from all cancer ROIs and all non-cancerous ROIs

were compared, 34 cancer-upregulated and 27 cancer-downregulated components were detected. Hence, we concluded that spectral components corresponding to lipid species could be detected that generally discriminate papillary thyroid cancer from non-cancerous thyroid tissue, not only normal healthy thyroid but also not neoplastic lesions.

Annotation of abundant components of registered spectra (i.e. spectral components with abundances higher than median) the LIPID MAPS database allowed hypothetical identification of 48 molecular species, which corresponded to $[M + H]^+$, $[M + Na]^+$ and $[M + K]^+$ ions of 22 lipids, including 12 phosphatidylcholines (PCs), 6 phosphatidic acids (PAs) and 4 sphingomyelins (SMs). In general, we observed the same molecular ions corresponding to lipid species in formalin-fixed and fresh-frozen thyroid tissue, yet sodium adducts were the most abundant in the former material whereas potassium adducts predominated in the latter type of material. Moreover, the abundance of registered ions was higher in fresh-frozen tissue (Supplementary Fig. s1). Hence, to verify the identity of detected lipids selected components were analysed by in tissue MS/MS in corresponding fresh-frozen cancerous tissue (Supplementary Fig. s2, Tab. sII). This analysis allowed the validation of the identity of 26 molecular ions.

Abundances of all 22 identified lipid species detected in thyroid tissue were compared pairwise in cancer and non-cancerous ROI for each patient separately (Table II). There were 13 lipid species (with 25 molecular ions) that showed cancer-upregulation in all 3 patients. Furthermore, increased abundance of 8 lipids in cancerous tissue was highly statistically significant, which included: phosphatidylcholines PC(32:0), PC(32:1), PC(34:1) and PC(36:3), phosphatidic acids PA(36:2) and PA(36:3), and sphingomyelins SM(34:1) and SM(36:1) (Fig. 2). This is noteworthy, in that several lipid species were not upregulated in cancerous thyroid when compared to colloid nodular goiter (Patient_1), which represents a benign thyroid neoplasm. Hence, these lipids did
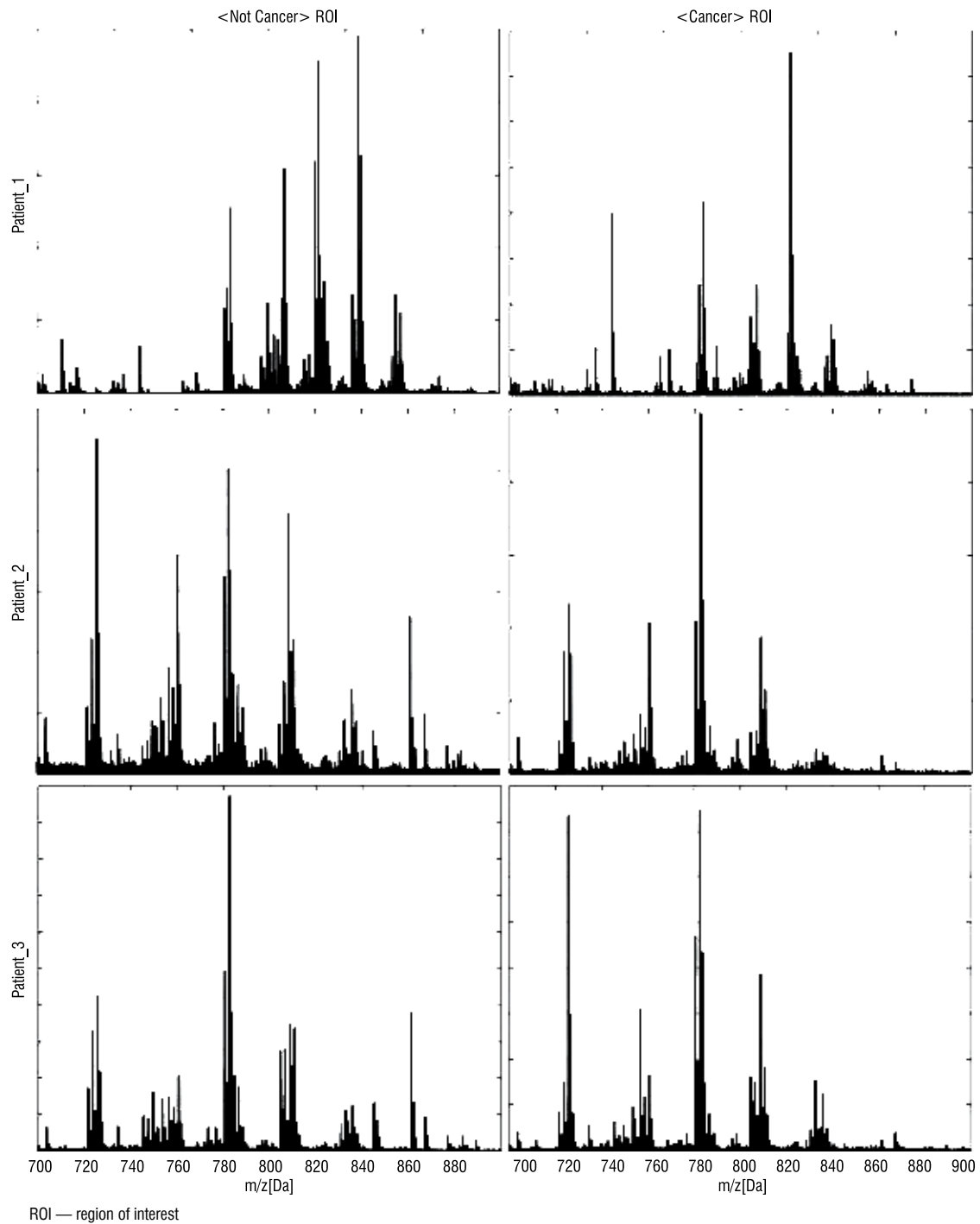
Figure 1. *Averaged mass spectra from cancerous and non-cancerous areas of thyroid tissue*

Rycina 1. *Uśrednione widma masowe z obszarów nowotworowych i nienowotworowych tkanek tarczycy*

not discriminate universally, PTC from non-cancerous thyroid. Lipids that were relatively downregulated in normal and inflammatory thyroid yet upregulated in nodular goiter included PC(36:2), PC(38:3), PC(38:4), PA(38:3), PA(38:5), SM(40:1) and SM(42:2).

A few papers have previously reported specific differences in lipid profiles between thyroid malignancies and non-cancerous thyroid, however in these studies chemically fixed tissue was not employed. Increased abundances of PC(34:1), PC(34:2) and SM(34:1) were observed in PTC when compared to healthy thyroid [17]. Moreover, PC(34:1), PA(36:3) and SM(34:1) could discriminate between thyroid cancers (PTC and FTC), benign thyroid neoplasms and normal thyroid [19]. Furthermore, increased levels of lipids with monounsaturated acyl chains relative to polyunsaturated lipid species were found to be characteristic of the thyroid cancer microenvironment [20].

Table II. *Identified lipids that differentiate PTC from non-cancerous thyroid tissue*

Tabela II. *Zidentyfikowane lipidy, które różnicują tkanki PTC od nienowotworowych tkanek tarczycy*

Compound	ion	registered m/z [Da]	Pt_1	Pt_2	Pt_3	Cancer/Non-cancerous ratio	Corrected p-value	Effect size
PC (32:0)	[M + H] $^+$	734.57	Up	Up	Up	1.94	<0.001	0.62
	[M + Na] $^+$	756.55	Up	Up	Up	1.70	<0.001	0.69
	[M + K] $^+$	772.53	Up	Up	Up	1.05	0.004	0.18
PC (32:1)	[M + Na] $^+$	754.54	Up	Up	Up	1.45	<0.001	0.52
	[M + K] $^+$	770.51	Up	Up	Up	1.21	<0.001	0.57
PC (34:1)	[M + H] $^+$	760.58	Down	Up	Up	1.22	<0.001	0.28
	[M + Na] $^+$	782.57	Up	Up	Up	1.31	<0.001	0.77
	[M + K] $^+$	798.54	Up	Up	Up	1.36	<0.001	0.51
PC (34:2)	[M + H] $^+$	758.57	Down	Up	Up	1.09	0.001	0.09
	[M + Na] $^+$	780.55	Up	Up	Up	1.03	0.012	0.17
	[M + K] $^+$	796.53	Up	Up	Up	1.29	<0.001	0.38
PC (36:1)	[M + H] $^+$	788.62	Down	Up	Up	0.84	0.001	0.26
	[M + Na] $^+$	810.59	Down	Up	Up	3.03	<0.001	0.07
	[M + K] $^+$	826.58	Up	Up	Up	0.98	0.437	0.03
PC (36:2)	[M + H] $^+$	786.60	Down	Up	Up	2.10	0.002	0.02
	[M + Na] $^+$	808.58	Down	Up	Up	0.78	<0.001	0.32
	[M + K] $^+$	824.56	Down	Up	Up	0.99	0.482	0.16
PC (36:3)	[M + H] $^+$	784.58	Up	Up	Up	1.18	<0.001	0.23
	[M + Na] $^+$	806.57	Down	Up	Up	0.82	0.344	0.08
	[M + K] $^+$	822.54	Up	Up	Up	1.18	<0.001	0.50
PC (36:4)	[M + Na] $^+$	804.55	Up	Up	Up	0.98	0.084	0.22
	[M + K] $^+$	820.52	Up	Up	Up	1.20	<0.001	0.44
PC (38:3)	[M + Na] $^+$	834.59	Down	Up	Up	0.76	0.376	0.01
PC (38:4)	[M + Na] $^+$	832.58	Down	Up	Up	0.73	0.004	0.16
	[M + K] $^+$	848.56	Down	Up	Up	0.98	0.441	0.03
PC (38:5)	[M + Na] $^+$	830.57	Down	Up	Up	0.75	0.454	0.01
	[M + K] $^+$	846.54	Up	Up	Up	0.92	<0.001	0.39
PC (38:6)	[M + K] $^+$	844.52	Up	Up	Up	0.99	0.131	0.11
PA (36:2)	[M + Na] $^+$	723.49	Up	Up	Up	1.14	<0.001	0.29
	[M + K] $^+$	739.47	Up	Up	Up	1.60	<0.001	0.91
PA (36:3)	[M + Na] $^+$	721.48	Down	Up	Up	2.69	0.022	0.15
	[M + K] $^+$	737.45	Up	Up	Up	1.48	<0.001	0.72
PA (38:3)	[M + Na] $^+$	749.51	Down	Up	Up	0.74	<0.001	0.56
PA (38:4)	[M + Na] $^+$	747.49	Up	Up	Up	1.04	0.231	0.01
	[M + K] $^+$	763.47	Up	Up	Up	0.94	<0.001	0.27
PA (38:5)	[M + Na] $^+$	745.48	Down	Up	Up	0.93	0.017	0.14
	[M + K] $^+$	761.45	Down	Up	Up	1.14	0.001	0.18
PA (40:5)	[M + H] $^+$	751.53	Down	Up	Up	0.77	<0.001	0.27
	[M + Na] $^+$	773.51	Down	Up	Up	0.84	<0.001	0.37
	[M + K] $^+$	789.48	Up	Up	Up	0.98	0.011	0.16
SM (40:1)	[M + Na] $^+$	809.65	Down	Up	Up	0.71	<0.001	0.23
SM (42:2)	[M + Na] $^+$	835.67	Down	Up	Up	0.90	0.001	0.24
	[M + K] $^+$	851.64	Down	Up	Up	0.94	0.010	0.16
SM (34:1)	[M + H] $^+$	703.57	Up	Up	Up	1.41	<0.001	0.50
	[M + Na] $^+$	725.58	Up	Up	Up	1.78	<0.001	1.01
	[M + K] $^+$	741.53	Up	Up	Up	1.58	<0.001	0.56
SM (36:1)	[M + Na] $^+$	753.59	Down	Up	Up	1.27	<0.001	0.54
	[M + K] $^+$	769.56	Up	Up	Up	0.99	0.837	0.11

Up and Down refers to relative upregulation and downregulation of compound in cancer ROI compare to matched non-cancerous ROI in subsequent patients (Pt_1, Pt_2, Pt_3); Cancer/Non-cancerous ratio (and corresponding statistical indices) refers to combined spectra from all Cancer ROIs and Non-cancerous ROIs
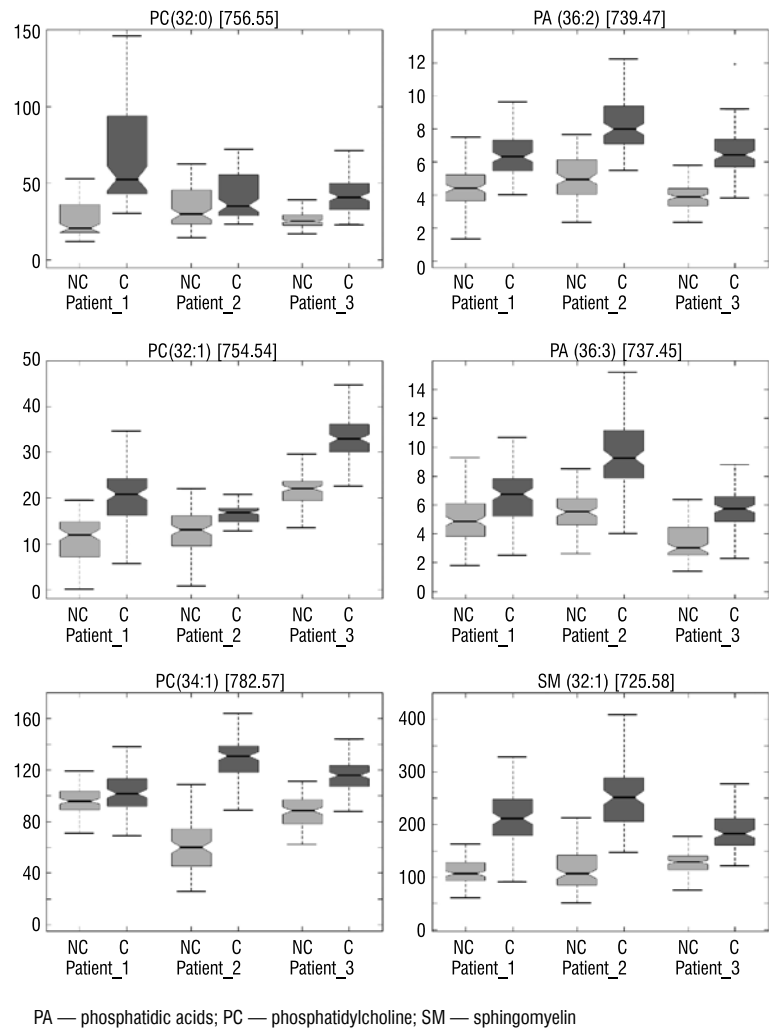
Figure 2. *Abundances of selected lipids in cancer and non-cancerous ROIs from three patients with PTC. Boxplots show minimum, lower quartile, median, upper quartile and maximum values*

Rycina 2. *Ilości wybranych lipidów z nowotworowych i nienowotworowych obszarów ROI pobranych od trzech pacjentów z PTC. Wykresy pokazują wartości minimalne, niższy kwartyl, mediany, górny kwartyl i wartości maksymalne*

PA — phosphatidic acids; PC — phosphatidylcholine; SM — sphingomyelin

Conclusions

Here we performed profiling of lipid species in formalin-fixed thyroid tissue, proving that this type of clinical material is compatible with mass spectrometry (MS)-based metabolomics/lipidomics studies. Several phosphatidylcholine, sphingomyelin and phosphatidic acid species were identified and quantified in analysed tissues. It was found that eight phospholipids, including PC(32:0), PC(32:1), PC(34:1), PC(36:3), PA(36:2), PA(36:3), SM(34:1) and SM(36:1), were upregulated in PTC and could be used to discriminate this malignancy from non-malignant thyroid tissue, either "normal" or benign neoplasm. This observation validated and further extended previous reports [17, 19]. Furthermore, several other lipid species that could putatively discriminate normal thyroid (either healthy or inflammatory) from benign thyroid neoplasms were detected. Hence, we confirmed that lipid profiling by MALDI-MSI could be potentially used for classification and differentiating diagnosis of thyroid diseases based on clinically relevant material (formalin-fixed tissue).

An advantage of this MSI approach in comparison to other MS-based analytical techniques lays in its unique ability to "extract" molecular information from small defined tissue regions. This is particularly helpful in cases where several distinct diseases co-exist within the same tissue specimen.

Ethics approval and consent to participate

Competing interests

The authors declare that they have no competing interests.

Funding

References

1. Cibas ES, Ali SZ. The Bethesda system for reporting thyroid cytopathology. Thyroid. 2009; 19: 1159–1165, doi: 10.1007/s12070-011-0289-4.
2. DeLellis RA, Lloyd RV, Heitz PU. Pathology and Genetics of Tumours of Endocrine Organs. WHO Classification of Tumours. IARC Press, Lyon 2004: Lyon.
3. Lloyd RV, Buehler D, Khanafshar E. Papillary thyroid carcinoma variants. Head Neck Pathol. 2011; 5(1): 51–56, doi: 10.1007/s12105-010-0236-9, indexed in Pubmed: 21221869.
4. Kakudo K, Kameyama K, Miyauchi A, et al. Introducing the reporting system for thyroid fine-needle aspiration cytology according to the new guidelines of the Japan Thyroid Association. Endocr J. 2014; 61(6): 539–552, doi: 10.1507/endocrj.ej13-0494, indexed in Pubmed: 24727657.
5. Faquin WC. The thyroid gland: recurring problems in histologic and cytologic evaluation. Arch Pathol Lab Med. 2008; 132(4): 622–632, doi: 10.1043/1543-2165(2008)132[622:TTGRPI]2.0.CO;2, indexed in Pubmed: 18384214.
6. Sakorafas GH. Thyroid nodules; interpretation and importance of fine-needle aspiration (FNA) for the clinician - practical considerations. Surg Oncol. 2010; 19(4): e130–e139, doi: 10.1016/j.suronc.2010.06.003, indexed in Pubmed: 20620044.
7. Jelonek K, Pietrowska M, Ros M, et al. Radiation-induced changes in serum lipidome of head and neck cancer patients. Int J Mol Sci. 2014; 15(4): 6609–6624, doi: 10.3390/ijms15046609, indexed in Pubmed: 24747595.
8. Fernandis AZ, Wenk MR. Membrane lipids as signaling molecules. Curr Opin Lipidol. 2007; 18(2): 121–128, doi: 10.1097/MOL.0b013e328082e4d5, indexed in Pubmed: 17353659.
9. Coussens LM, Werb Z. Inflammation and cancer. Nature. 2002; 420(6917): 860–867, doi: 10.1038/nature01322, indexed in Pubmed: 12490959.
10. Gschwind A, Prenzel N, Ullrich A. Lysophosphatidic acid-induced squamous cell carcinoma cell proliferation and motility involves epidermal growth factor receptor signal transactivation. Cancer Res. 2002; 62(21): 6329–6336, indexed in Pubmed: 12414665.
11. Dória ML, Cotrim Z, Macedo B, et al. Lipidomic approach to identify patterns in phospholipid profiles and define class differences in mammary epithelial and breast cancer cells. Breast Cancer Res Treat. 2012; 133(2): 635–648, doi: 10.1007/s10549-011-1823-5, indexed in Pubmed: 22037781.
12. Fernandis AZ, Wenk MR. Lipid-based biomarkers for cancer. J Chromatogr B Analyt Technol Biomed Life Sci. 2009; 877(26): 2830–2835, doi: 10.1016/j.jchromb.2009.06.015, indexed in Pubmed: 19570730.
13. Ishikawa S, Tateya I, Hayasaka T, et al. Increased expression of phosphatidylcholine (16:0/18:1) and (16:0/18:2) in thyroid papillary cancer. PLoS One. 2012; 7(11): e48873, doi: 10.1371/journal.pone.0048873, indexed in Pubmed: 23139822.
14. Ryu J. Lipid MALDI MS Profiling Accurately Distinguishes Papillary Thyroid Carcinoma from Normal Tissue. Journal of Proteomics & Bioinformatics. 2013; 06(04), doi: 10.4172/jpb.1000263.
15. Guo S, Qiu L, Wang Y, et al. Tissue imaging and serum lipidomic profiling for screening potential biomarkers of thyroid tumors by matrix-assisted laser desorption/ionization-Fourier transform ion cyclotron resonance mass spectrometry. Anal Bioanal Chem. 2014; 406(18): 4357–4370, doi: 10.1007/s00216-014-7846-0, indexed in Pubmed: 24842401.
16. Guo S, Wang Y, Zhou D, et al. Significantly increased monounsaturated lipids relative to polyunsaturated lipids in six types of cancer microenvironment are observed by mass spectrometry imaging. Sci Rep. 2014; 4: 5959, doi: 10.1038/srep05959, indexed in Pubmed: 25091112.
17. Caprioli RM, Farmer TB, Gile J. Molecular imaging of biological samples: localization of peptides and proteins using MALDI-TOF MS. Anal Chem. 1997; 69(23): 4751–4760, doi: 10.1021/ac970888i, indexed in Pubmed: 9406525.
18. Schwamborn K, Caprioli RM. Molecular imaging by mass spectrometry-looking beyond classical histology. Nat Rev Cancer. 2010; 10(9): 639–646, doi: 10.1038/nrc2917, indexed in Pubmed: 20720571.
19. Seeley EH, Caprioli RM. MALDI imaging mass spectrometry of human tissue: method challenges and clinical perspectives. Trends Biotechnol. 2011; 29(3): 136–143, doi: 10.1016/j.tibtech.2010.12.002, indexed in Pubmed: 21292337.
20. Clench MR. Advances in mass spectrometry imaging. Proteomics. 2016; 16(11-12): 1605–1606, doi: 10.1002/pmic.201600202, indexed in Pubmed: 27303928.
21. Fox CH, Johnson FB, Whiting J, et al. Formaldehyde fixation. J Histochem Cytochem. 1985; 33(8): 845–853, doi: 10.1177/33.8.3894502, indexed in Pubmed: 3894502.
22. Hackett MJ, McQuillan JA, El-Assaad F, et al. Chemical alterations to murine brain tissue induced by formalin fixation: implications for biospectroscopic imaging and mapping studies of disease pathogenesis. Analyst. 2011; 136(14): 2941–2952, doi: 10.1039/c0an00269k, indexed in Pubmed: 21629894.
23. Pietrowska M, Gawin M, Polańska J, et al. Tissue fixed with formalin and processed without paraffin embedding is suitable for imaging of both peptides and lipids by MALDI-IMS. Proteomics. 2016; 16(11-12): 1670–1677, doi: 10.1002/pmic.201500424, indexed in Pubmed: 27001204.
24. Initializing EM algorithm for univariate Gaussian, multi-component, heteroscedastic mixture models by dynamic programming partitions. arXiv:1506.07450v2 [stat.AP] 2015.

PRACE ORYGINALNE